Master equations for quantum transport with Franck-Condon blockade

Hannes Hübener[1,2] and Tobias Brandes[3]
[1]*Laboratoire des Solides Irradiés, École Polytechnique, CNRS–CEA/DSM, 91128 Palaiseau, France*
[2]*European Theoretical Spectroscopy Facility (ETSF)*
[3]*Institut für Theoretische Physik, Technische Universität Berlin, 10623 Berlin, Germany*
(Received 23 July 2009; revised manuscript received 25 September 2009; published 19 October 2009)

The Master equation framework for single electron transport is extended to include the Franck-Condon effect that can dominate the transport properties of nanoelectromechanical devices. The quantum nature of the resulting vibroelectronic states leaves a signature in the electronic shot noise, which is accounted for by careful treatment of the coherences. Two model systems are shown to demonstrate the relevance of such a formulation.

DOI: 10.1103/PhysRevB.80.155437 PACS number(s): 73.23.Hk, 73.63.Kv

I. INTRODUCTION

Master equations for electronic transport through mesoscopic devices are a well established tool to describe charge,[1] spin,[2] and quantum coherence[3–5] effects in nanostructures. Recently, with the emergence of nanoelectromechanical (NEMS) devices,[6–11] Master equations have been used to describe the dynamics of electron transport where the electronic and mechanical degrees of freedom are coupled, leading to new effects such as the Franck-Condon (FC) blockade[12–14] or quantum shuttling.[15–18]

The FC effect in such systems refers to the modifications of electronic transition rates due to the overlap of initial and final vibrational state in an analogous way to the FC principle of molecular physics[19] and can lead to a complete suppression of transport when these states are orthogonal. It is thus necessary to incorporate the FC effect into the Master equation formalism when considering single electron transport in NEMS.

The study of NEMS allows the observation of quantum coherent behavior of objects (molecules or mechanical resonators) that are big on the scale of smaller units (electrons, atoms) and thus provide an intriguing way of realizing macroscopic quantum mechanical effects. The signature of quantum mechanical behavior is coherent interaction between two states, which for single electron transport can be observed as a resonance in the electronic noise spectrum.[20] This behavior can only be accounted for by considering the full density operator of the system, i.e., keeping all coherences in the Master equation.

In this paper, we describe in detail the derivation of a FC Master equation with all coherences as well as its application to example systems, where the mentioned features occur. In our derivation, the overlap integrals between the initial and final vibrational state of a tunneling event that modify the transition rates follow from a careful treatment of the vibroelectronic states. We then apply this Master equation to a nanomechanical system, where the full account of the coherences is crucial to observe an electronic finger print of coherent tunneling of the vibrational states. Also, we investigate the dependence of the steady state coherences on damping of the system. Furthermore, we propose another system where this electronic finger print and its absence reveals an interesting insight into the inner dynamics of a system under FC blockade conditions.

II. FRANCK-CONDON MASTER EQUATION

The general set-up we consider for vibrational assisted transport is that of a small vibrational-electronic system weakly coupled to two electronic reservoirs (left and right), such that the Master equation formalism can be applied. Here, we discuss a form of Master equation that especially accounts for the coherences and vibrational degrees of freedom of a NEMS. The Hamiltonian can be written as a sum of the system Hamiltonian, the reservoir Hamiltonians and the Hamiltonian that accounts for the coupling between them

$$H = H_{\mathrm{sys}} + H_{\mathrm{Res}} + H_{\mathrm{T}}. \tag{1}$$

Transport is assumed to take place under Coulomb blockade conditions, therefore it is sufficient to treat only one additional electron on the dot. The eigenstates of the system depend on a vibrational and an electronic quantum number. We denote the states as $|n,\nu\rangle = |n\rangle_{\mathrm{vib}} \otimes |\nu\rangle_{\mathrm{el}}$ where $\nu \in \{0,1\}$. It is important to note that the vibrational part of these states depends also on the electronic quantum number, because the electronic content of the system changes its potential and consequently the vibrational eigenfunctions change with the electronic content. To take this into account when dealing with the vibrational parts only, we will write the corresponding electronic quantum number as an index to the vibrational kets: $|n,\nu\rangle \equiv |n\rangle_{\nu} \otimes |\nu\rangle_{\mathrm{el}}$.

It is assumed that the eigenvalue problem of the system Hamiltonian is solved, so that it can be represented as

$$H_{\mathrm{sys}} = \sum_i \varepsilon_{1,i} |i,1\rangle\langle i,1| + \sum_j \varepsilon_{0,j} |j,0\rangle\langle j,0|, \tag{2}$$

where we treat the number of states of the charged system independently from the number of states of the uncharged system, hence the two sums. The reservoir Hamiltonians can be written as

$$H_{\mathrm{Res}} = \sum_{k_{L,R}} \varepsilon_k c_k^{\dagger} c_k. \tag{3}$$

The coupling of the system to the reservoirs is a purely electronic process, therefore we define creation and annihilation operators of the electronic states of the system

$$d^\dagger = |1\rangle_{\text{el}\ \text{el}}\langle 0| \quad d = |0\rangle_{\text{el}\ \text{el}}\langle 1|. \tag{4}$$

With these system operators the coupling can be modeled according to

$$H_{\text{T}} = \sum_{k_{L,R}} V_k (c_k^\dagger d + d^\dagger c_k). \tag{5}$$

We take this Hamiltonian to define an interaction picture, with the free Hamiltonian $H_0 = H_{\text{Res}} + H_{\text{sys}}$. The Liouville-von Neuman equation in this interaction picture reads

$$\dot{\tilde{\chi}}(t) = -i[\tilde{H}_{\text{T}}(t), \tilde{\chi}(t)]. \tag{6}$$

Tracing out reservoir states and performing perturbation to second order yields

$$\dot{\tilde{\rho}}(t) = -\int_0^t \text{Tr}_{\text{Res}}\{[\tilde{H}_{\text{T}}(t), [\tilde{H}_{\text{T}}(t'), \tilde{\chi}(t')]]\}, \tag{7}$$

where also the initial condition $\text{Tr}_{\text{Res}}\{[\tilde{H}_{\text{T}}(0), \tilde{\chi}(0)]\} = 0$ is assumed. Expanding the commutators leads with some straightforward algebra to the Master equation in interaction picture[3]

$$\begin{aligned}
\dot{\tilde{\rho}}(t) = &-\sum_{k_{L,R}} \int_0^t dt' |T_k|^2 f(\varepsilon_k) e^{i\varepsilon_k(t-t')} [\tilde{d}(t)\tilde{d}^\dagger(t')\tilde{\rho}(t') - \tilde{d}^\dagger(t')\tilde{\rho}(t')\tilde{d}(t)] \\
&-\sum_{k_{L,R}} \int_0^t dt' |T_k|^2 (1 - f(\varepsilon_k)) e^{-i\varepsilon_k(t-t')} [\tilde{d}^\dagger(t)\tilde{d}(t')\tilde{\rho}(t') - \tilde{d}(t')\tilde{\rho}(t')\tilde{d}^\dagger(t)] \\
&-\sum_{k_{L,R}} \int_0^t dt' |T_k|^2 f(\varepsilon_k) e^{-i\varepsilon_k(t-t')} [\tilde{\rho}(t')\tilde{d}(t')\tilde{d}^\dagger(t) - \tilde{d}^\dagger(t)\tilde{\rho}(t')\tilde{d}(t')] \\
&-\sum_{k_{L,R}} \int_0^t dt' |T_k|^2 (1 - f(\varepsilon_k)) e^{i\varepsilon_k(t-t')} [\tilde{\rho}(t')\tilde{d}^\dagger(t')\tilde{d}(t) - \tilde{d}(t)\tilde{\rho}(t')\tilde{d}^\dagger(t')],
\end{aligned} \tag{8}$$

where $f(\varepsilon)$ are the Fermi functions. The important step, in which this derivation differs from others, is to now take matrix elements of this equation in the eigenbasis of the system. This amounts to taking the matrix elements of the eight different terms in Eq. (8). The first one, for example, reads

$$\langle n,\nu|\tilde{d}_t \tilde{d}^\dagger_{t'} \tilde{\rho}_{t'}|m,\mu\rangle = \sum_{i,j} \langle n,\nu|\tilde{d}_t|i,1\rangle\langle i,1|\tilde{d}^\dagger_{t'}|j,0\rangle\langle j0|\tilde{\rho}_{t'}|m,\mu\rangle \tag{9}$$

$$= \sum_{i,j} \exp\{i(\varepsilon_{0n}t - \varepsilon_{1i}t + \varepsilon_{1i}t' - \varepsilon_{0j}t')\}_0\langle n|i\rangle_{1\ 1}\langle i|j\rangle_0 \delta_{\nu 0}\langle j,0|\tilde{\rho}_{t'}|m,\mu\rangle, \tag{10}$$

and the other terms are treated similarly. Before transforming back into the Schrödinger picture, we carry out the Markov approximation, which means we replace $\tilde{\rho}(t') \to \tilde{\rho}(t)$ under the integral and which also allows us to replace the integral $\int_0^t dt' \to \int_{-\infty}^{\infty} dt'$.[28] The transformation to the Schrödinger picture is done according to

$$\frac{d}{dt}\rho(t) = -i[H_0, \rho] + e^{-iH_0 t}\frac{d}{dt}\tilde{\rho}_t e^{iH_0 t}. \tag{11}$$

This finally yields our FC Master equation

$$\begin{aligned}
\frac{d}{dt}\langle n,\nu|\rho(t)|m,\mu\rangle = &-i(\varepsilon_{\nu n} - \varepsilon_{\mu m})\langle n,\nu|\rho_t|m,\mu\rangle \\
&-\sum_{\substack{\alpha=L,R \\ i,j,i',j'}} \{\gamma_\alpha(\varepsilon_{1i} - \varepsilon_{0j'})\tau_{in}\tau_{ij'}\langle j',0|\rho_t|m,\mu\rangle\delta_{\nu 0} - \gamma_\alpha(\varepsilon_{1n} - \varepsilon_{0j})\tau_{nj}\tau_{mj'}\langle j,0|\rho_t|j',0\rangle\delta_{\nu 1}\delta_{\mu 1} \\
&+ \bar{\gamma}_\alpha(\varepsilon_{1i'} - \varepsilon_{0j})\tau_{nj}\tau_{i'j}\langle i',1|\rho_t|m,\mu\rangle\delta_{\nu 1} - \bar{\gamma}_\alpha(\varepsilon_{1i} - \varepsilon_{0n})\tau_{in}\tau_{i'm}\langle i,1|\rho_t|i',1\rangle\delta_{\nu 0}\delta_{\mu 0} \\
&+ \gamma_\alpha(\varepsilon_{1i'} - \varepsilon_{0j})\tau_{i'j}\tau_{i'm}\langle n,\nu|\rho_t|j,0\rangle\delta_{\mu 0} - \gamma_\alpha(\varepsilon_{1m} - \varepsilon_{0j'})\tau_{nj}\tau_{mj'}\langle j,0|\rho_t|j',0\rangle\delta_{\nu 1}\delta_{\mu 1} \\
&+ \bar{\gamma}_\alpha(\varepsilon_{1i} - \varepsilon_{0j'})\tau_{ij'}\tau_{mj'}\langle n,\nu|\rho_t|i,1\rangle\delta_{\mu 1} - \bar{\gamma}_\alpha(\varepsilon_{1i'} - \varepsilon_{0m})\tau_{in}\tau_{i'm}\langle i,1|\rho_t|i',1\rangle\delta_{\nu 0}\delta_{\mu 0}\},
\end{aligned} \tag{12}$$

where the summation is only over two common pairs of the four indices i,j,i',j' in each term and we defined the rates $\gamma_\alpha(\varepsilon)=\Gamma_\alpha f_\alpha(\varepsilon)$ for tunneling onto the dot and $\bar{\gamma}_\alpha(\varepsilon)=\Gamma_\alpha[1-f_\alpha(\varepsilon)]$ for tunneling off the dot. The tunneling coupling strength is defined as $\Gamma_\alpha=2\pi\nu_\alpha(\varepsilon)=2\pi\Sigma_k|T_k|^2\delta(\varepsilon-\varepsilon_k)$.

When deriving the Master equation for such a system with vibrational and electronic degrees of freedom as outlined above, one encounters nonzero overlaps of the form $\tau_{ij}={}_1\langle i|j\rangle_0$, which are the FC factors, well-known from molecular quantum mechanics:[19]

$$\tau_{ij}=\int_0^\infty dx\psi_{i1}(x)\psi_{j0}(x). \tag{13}$$

It is an important feature of our derivation of the Master equation that these factors occur naturally and do not need to be included using phenomenological arguments.

We would like to stress two important points regarding this form of a Master equation. First, we note that all coherences have been retained, to account for the full coherent behavior of the system, thus arriving at a somewhat different result than the canonical Master equation. However, under the assumptions that the coherences are zero, Eq. (12) yields the matrix elements of a Lindblad form Master equation. Those coherences that are not diagonal with respect to the electronic quantum number decouple from the rest of the Master equation, i.e., $\langle n,0|\rho|m,1\rangle=\langle n,1|\rho|m,0\rangle=0$. Second, we point out that the FC factors generally do not enter as squared values, which is usually the case in approaches using rate equation or Lindblad form Master equations.[12,14] Instead, our derivation yields products of different FC factors, so that their sign becomes important. That means the factors modulating the transition amplitudes of coherences can be negative, while for the populations, the factors are squared values in accordance with the other approaches.

III. EXAMPLE SYSTEMS

A. Model I

We now apply the Master equation (12) to a model where its full account of the coherences is the crucial point to detect coherent dynamics within the system. The model is a single mode oscillating nanostructure realized in several experiments either as a molecule,[6,21] a carbon nanotube,[22–24] or as an etched GaAs nanoscale rod.[25] We describe the electronic properties of the system as a single level quantum dot. The electronic coupling to the environment, namely, a gate or a substrate, leads to an image charge effect when the dot is in an occupied state. We model this system with the Hamiltonian

$$H=\frac{\mathbf{P}^2}{2M}+\frac{1}{2}M\omega_0^2(\mathbf{a}-\mathbf{r})^2-d^\dagger d\frac{e^2}{4\pi\epsilon_0}\frac{1}{2\mathbf{r}\cdot\hat{\mathbf{u}}}, \tag{14}$$

where $\mathbf{a}$ is the equilibrium position of the harmonic vibration, so that the origin is on the surface where the image charge of the dot electron forms (cf. Figure 1). The unit vector $\hat{\mathbf{u}}$ points in the direction perpendicular to this plane. We note that a similar Hamiltonian has been used to model a two electron system on a quantum, the so-called quantum dot Helium.[30,31]

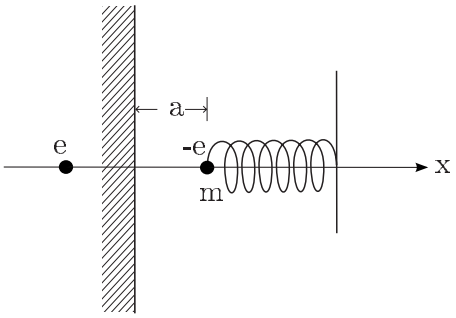

FIG. 1. Schematic model of the considered system: a vibrating structure with a single electron quantum dot near a plane where an image charge effect occurs.

The various parameters of the model can be combined to the two dimensionless parameters

$$\Omega\equiv\frac{M\omega_0}{\hbar}a^2=\frac{a^2}{l_0^2},\quad \epsilon\equiv\frac{e^2Ma}{8\hbar^2\pi\varepsilon_0\varepsilon_r}=\Omega\frac{E_a}{\hbar\omega_0}. \tag{15}$$

The parameter Ω relates the oscillator length l_0 to the distance of the system to the surface and thus controls the shape of the potential for the uncharged dot. The parameters ϵ is the scaled Coulomb coupling of the dot electron with the environment

$$E_a\equiv\frac{e^2}{4\pi\varepsilon_0\varepsilon_r 2a}. \tag{16}$$

Considering only the direction perpendicular to the plane, we can rewrite the system Hamiltonian as the dimensionless operator

$$H=-\frac{1}{2}\frac{\partial^2}{\partial x^2}+\frac{\Omega^2}{2}(1-x)^2-d^\dagger d\frac{\epsilon}{x}. \tag{17}$$

1. Potentials and wave functions

There are two different potentials for this system, depending on the electronic content of the dot. When the dot is empty, the potential is just the harmonic potential shifted by the distance $a=|\mathbf{a}|$ with the eigenstates denoted $|n,0\rangle$ (cf. Sec. II for notation). When the dot is charged, however, the system potential is a superposition of this harmonic potential and the Coulomb potential of the image charge as shown in Fig. 2. We note the resemblance of the system Hamiltonian (14) to the Hamiltonian of the Hydrogen atom for the s orbital. We use this similarity in order to express the Hamiltonian in the basis of the Hydrogen eigenstates, which are the Laguerre functions Eq. (A1) (cf Appendix) and we are thus able to exactly solve the system by numerical diagonalization.

The eigenvalue spectrum (Fig. 3) as a function of the oscillator parameter Ω shows the two characteristics of its underlying potential. For $\Omega=0$, the eigenvalues have the $1/n^2$ spacing of hydrogen atom eigenstates. For increasing Ω, i.e., an increasing contribution of the harmonic term to

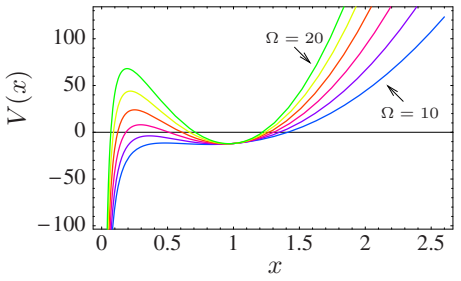

FIG. 2. (Color online) Potential of the charged system for different parameters $\Omega \in \{10,12,14,16,18,20\}$. Near the origin, the potential has a hydrogen-potential-like shape, while for larger x values the shape of the harmonic potential dominates. With increasing Ω, the harmonic character becomes more pronounced at small x values, leading to a potential well, with minimum around $x=1$.

the potential, the spectrum approaches the fan like structure, which is typical for harmonic oscillator spectra.

Another important feature of the spectrum is the occurrence of level anticrossing, which points toward coherent interaction between the two states. This is supported by the shape of the wave functions shown in Fig. 4. The wave functions are mainly localized either to the left, where the potential has the hydrogen-like singularity, or to the right (harmonic potential). The comparison between the first and the second eigenfunctions suggests that the eigenstates are bonding/antibonding superpositions of a "left" and a "right" state, similar to the two-level eigenbasis. In this way, the potential of the charged electrovibrational system (Fig. 2) allows for states to be formed as superpositions of states like the hydrogen ground state and harmonic oscillator-like ground states. This superposition would be accompanied by coherent oscillation between these two states that are predominantly localized in a left/right regime. This picture is supported by the occurrence of level anticrossing in the eigenvalue spectrum of the Hamiltonian of the charged system, Fig. 3. From the two-level system, it is known that indeed level anticrossing is a feature of two coherently interacting quantum states.

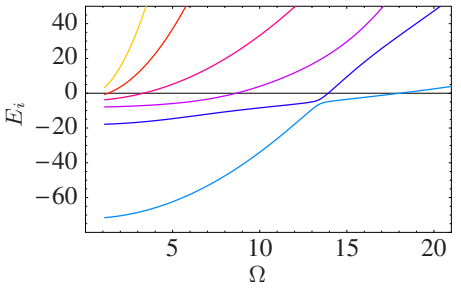

FIG. 3. (Color online) Eigenvalue spectrum of the Hamiltonian (14) for $\epsilon=12$ as a function of the oscillator parameter Ω, showing the six lowest eigenvalues. For $\Omega \to 0$, the spectrum has the $1/n^2$ characteristic of the Hydrogen atom, while for large Ω, the spectrum assumes the fanlike shape typical for harmonic spectra. At intermediate values of Ω, we observe a level repulsion between the first and the second level.

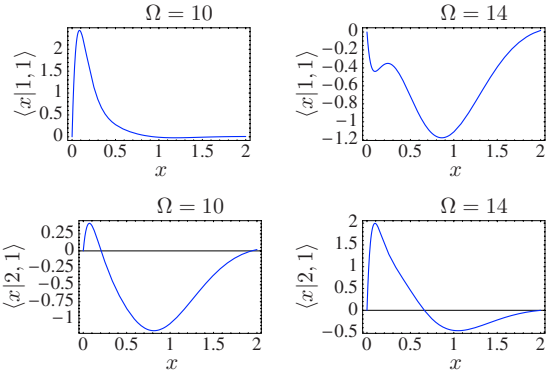

FIG. 4. (Color online) The first two Eigenfunctions of the Hamiltonian (14) for values of the oscillator parameter Ω before and after the level anticrossing. The two wave functions exchange their characteristics at this point, while keeping the properties of the first and second state.

We use the exact eigenfunctions $|n,1\rangle$ of the charged system and the harmonic oscillator eigenstates of the uncharged system to compute the FC factors according to Eq. (13). As mentioned above, these transition amplitudes can assume negative values and indeed Fig. 5 shows even oscillating behavior of some FC factors as functions of Ω, which means that they vanish for certain Ω values. This leads to a suppression of a transport channel that has been called FC blockade.[12,14]

2. Damping, coherences, & noise

Damping of the system is modeled by rewriting the Hamiltonian

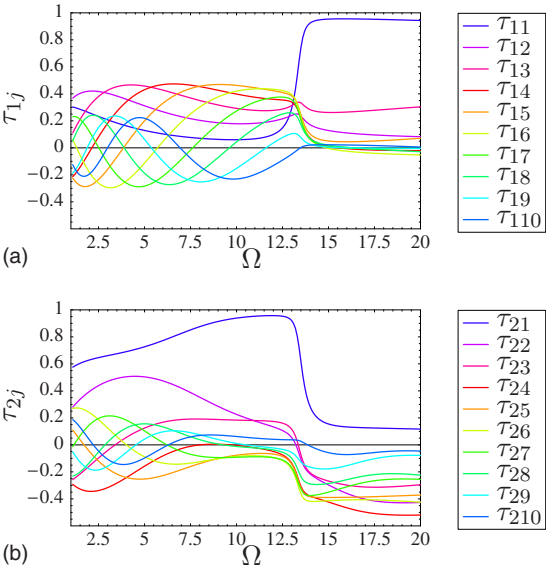

FIG. 5. (Color online) FC factors $\tau_{1,j}$ and $\tau_{2,j}$ as functions of the oscillator parameter Ω, which modify the transition rates between the charged and the uncharged oscillator states. We note that they can assume negative values and even vanish for certain Ω values, thus blocking the corresponding transition.

$$H = \omega_0 a^\dagger a - d^\dagger d \frac{e^2}{4\pi\epsilon_0} \frac{1}{2\mathbf{r}\cdot\hat{\mathbf{u}}} \tag{18}$$

and coupling a bosonic bath to the vibrational operators $a^\dagger$ and a, which under rotating wave approximation leads to a Lindblad form Master equation

$$\dot{\rho}(t) = -\frac{\gamma}{2}(a^\dagger a\rho + \rho a^\dagger a - 2a\rho a^\dagger), \tag{19}$$

which is additive with the electronic transport Master equation (12).

We couple this system to two leads as described in Sec. II. Here, we concentrate on those parameter values where the anticrossing occurs in the spectrum, e.g., $\epsilon=12$ and $9<\Omega<17$. For these parameters, it is reasonable to consider only the two lowest eigenstates of the system, since the separation to the next higher level is on the order of one magnitude larger than the level spacing in the level repulsion region. For the uncharged system such argument does not apply, since we are dealing with an equally spaced harmonic oscillator spectrum. So in this case, truncation of the Hilbert space has to be justified by numerical arguments, such the results converge as a function of the basis size. We found that a number of 10 uncharged oscillator states is reasonable.

To calculate the current and the current noise, we define the quantum jump operator, that is equivalent to the current operator within the Master equation framework.[26] Defining the Master equation with a Liouvillian superoperator $\dot{\rho}(t) = \mathcal{L}\rho(t)$ the Liouvillian can be split into two parts: $\mathcal{L}=L_0+\mathcal{L}_J$, where $\mathcal{L}_J$ is the part of the Master equation that accounts for the transitions at the left (right) lead and is therefore defined to be the quantum jump generator. $\mathcal{L}_0=\mathcal{L}-L_J$ is the remaining part of the Liouvillian. This means in Eq. (8), we identify the terms that contain $\tilde{d}^\dagger\tilde{\rho}\tilde{d}$ and $\tilde{d}\tilde{\rho}\tilde{d}^\dagger$ and keep track of them through the derivation of the Master equation, so that we know to which terms they correspond in the final form of the FC Master equation. The current and the current noise are then readily calculated from

$$I = \langle\langle 0|\mathcal{L}_J|0\rangle\rangle \tag{20}$$

$$S(\omega) = I - 2\,\mathrm{Re}[\langle\langle 0|\mathcal{L}_J\mathcal{R}(\omega)\mathcal{L}_J|0\rangle\rangle], \tag{21}$$

where $\langle\langle 0|\bullet|0\rangle\rangle = \mathrm{Tr}[1\bullet\rho_{\mathrm{stat}}]$, with ρ_{stat} being the stationary solution of the Master equation.[27]

3. Results

In Fig. 6, we show the calculated noise spectrum for several parameters. Comparison to the eigenvalue spectrum (Fig. 3) shows the sensitivity of the frequency dependent noise to the level anticrossing. We observe a resonant peak in the noise at those frequencies that correspond to the energy difference of the eigenvalues. Furthermore, the height of this peak greatly depends on the level anticrossing, reaching its maximum when the levels are closest and vanishing completely for Ω values away from the anticrossing point. This is a clear indicator for increased internal dynamics due to level coupling. Consequently, we interpret this behavior of the electronic noise spectrum as a fingerprint of coherent tunneling between the two vibrational states.

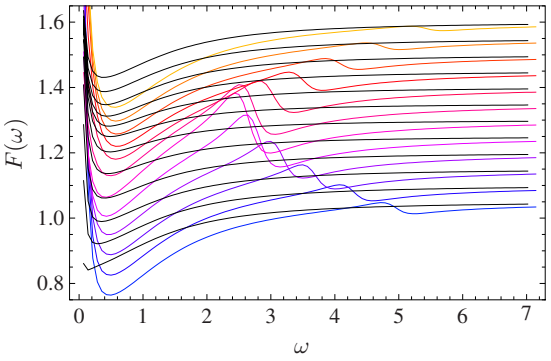

FIG. 6. (Color online) Frequency-dependent Fano factor $F(\omega)=S(\omega)/I$ for systems with finite bias $V_{\mathrm{Bias}}=\mu_L-\mu_R=40$ and asymmetric tunneling coupling $\Gamma_L=1/(2\pi)=2\Gamma_R$ and different oscillator parameters $\Omega=13$ (lowest line) to $\Omega=14.2$ (highest line), which is the interval in which the level anticrossing in the eigenvalue spectrum occurs ($\Omega\approx 13.6$). The labels refer to the lowest line, all other lines have an offset of $0.05n$. The colorful lines are results obtained using the FC Master equation (Eq. (12)), while the black lines are the corresponding results from a calculation where all coherences are set to zero.

In the calculations shown in Fig. 6, the coherences of the steady state density operator all vanish. We would like to point out, however, that this feature of the noise spectrum cannot be found if one uses a simple rate equation approach or a Lindblad form Master equation, as shown in Fig. 6 (black lines), which shows a calculation where all coherences are set to zero. It is the retaining of the full coherences as we did in deriving our Master equation that enables us to account for the coherence effects in the noise, although they are zero in the steady state case.

The situation changes, however, if we include damping of the oscillator as described above. In this case, we find finite coherences already in the steady state. Figure 7 shows several examples: the general trend is that coherences are small compared to the populations, but the average over all coherences grows as a function of the mechanical damping. The two dissipation mechanism, escape of electrons at rate $\bar{\gamma}_\alpha$ and mechanical damping at rate γ, thus compete with each other: the energy eigenbasis selected by pure electronic damping is no longer the preferential "pointer state" basis if mechanical damping [which refers to the uncharged oscillator basis, cf. Eq. (19)] is also present.

B. Model II

To further illustrate how our Master equation accounts for the subtle interplay between coherences and FC factors when considering current noise, we introduce another model that can be seen as a variation in the first model. We propose a system where a vibrating nanostructure interacts with two image charges as a result of a charging process. The axis along which the two image charges act on the oscillator is perpendicular to the direction of electron transport, to rule

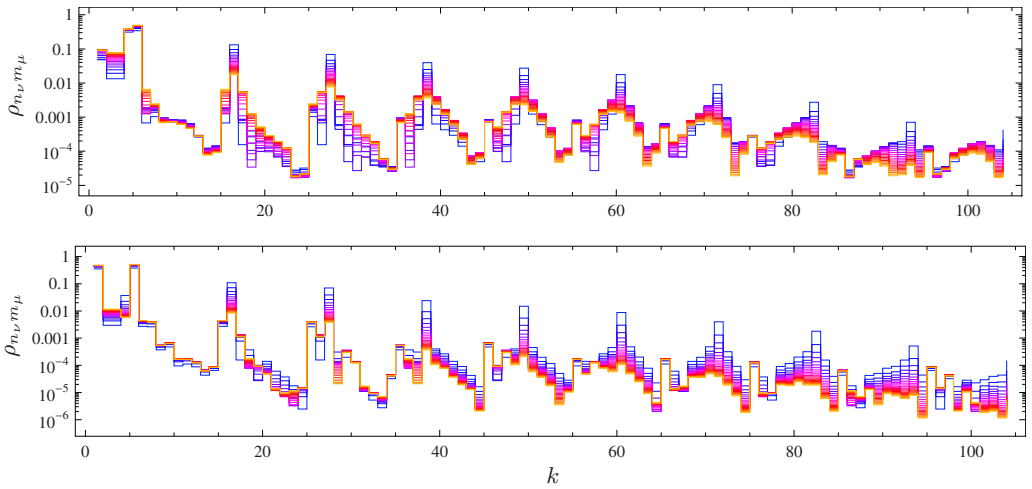

FIG. 7. (Color online) Moduli of steady state solutions of the FC Master equation (12) for $\epsilon=12$ and $\Omega=11$ (top) and $\Omega=15$ (bottom) with 20 different values of the damping parameter γ in the interval (0,10]. The scale goes from blue (black) through red (gray) to yellow (light gray). The four indices of the matrix elements of the Master equation are mapped to the one index k via $k=\delta_{\nu,1}[2(n-1)+m]+\delta_{\nu,0}[4+10(n+1)+m]$, which means that the equally spaced peaks refer to the populations of the uncharged oscillator states and the peaks at $k=1$ and $k=4$ are the populations of the charged states. We observe that the coherences are all smaller than the populations and that with increasing damping the populations of the higher uncharged states vanish as well as their coherences. Some coherences, however, *increase* with increasing damping, leading to an increase in the coherences on average.

out shuttle effects, cf. Fig. 8. In the uncharged state, the system is a normal harmonic oscillator, but when it is charged with an electron the effect of the two image charges is such that its potential has two singularities at the location of two scanning tunnel microscope (STM) tips. Here, we do not use the STM tips to probe the system, but simply as a means of applying metallic "electron-mirrors" in a controlled way. The harmonic potential of the uncharged oscillator is thus reduced to a local minimum at the position of the equilibrium in the uncharged state, Fig. 9.

The Hamiltonian of the charged system now reads, analogously to our previous formulation [cf. Eq. (17)]

$$H = -\frac{1}{2}\frac{\partial^2}{\partial x^2} + \frac{\Omega}{2}(x-1)^2 + d^\dagger d\left(\frac{\varepsilon}{x-2\pi} - \frac{\varepsilon}{x}\right). \tag{22}$$

Since the charged system is only defined for $x \in (0, 2\pi)$, this system is very similar to the basic quantum mechanics example of a particle in the infinite potential box, only that here, we have some interesting potential (Fig. 9) inside the box. Therefore, it is convenient to diagonalize this Hamiltonian in the basis of sine-functions

$$\phi_k(x) = \frac{1}{\sqrt{\pi}}\sin\frac{k}{2}x. \tag{23}$$

It turns out that this basis is very efficient, so that convergence of the eigenvalues with respect to basis size is easily reached with a set of 100 basis functions.

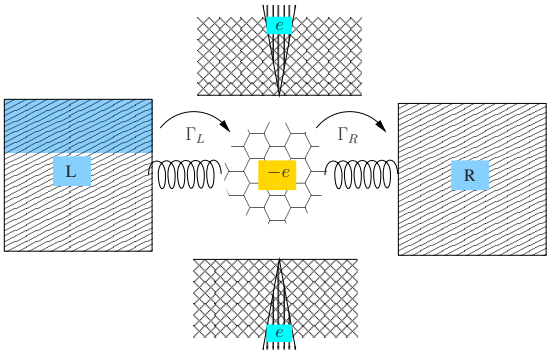

FIG. 8. (Color online) The proposed model. The structure is suspended with contacts to a source (l) and drain (r), while it experiences, in its charged state ($-e$), the images charges of two metallic STM tips (e), which are symmetrically applied perpendicular to the transport direction (Γ_L,Γ_R).

1. Spectrum and wave functions

The spectrum of H [Eq. (22)] Fig. 10 shows level anticrossings and in general the same characteristics as in our

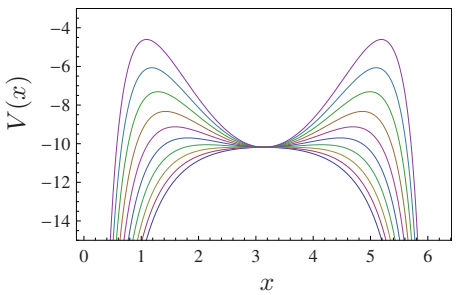

FIG. 9. (Color online) Potential of the Hamiltonian (22) for $\varepsilon=16$ and various values for Ω between 1 and 2.5.

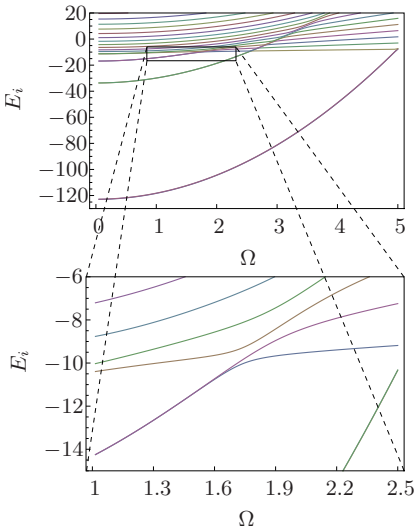

FIG. 10. (Color online) Spectrum of the Hamiltonian (22) for the Coulomb parameter $\varepsilon=16$. Low lying states are pairwise degenerate before they experience level anticrossing with the next higher lying state.

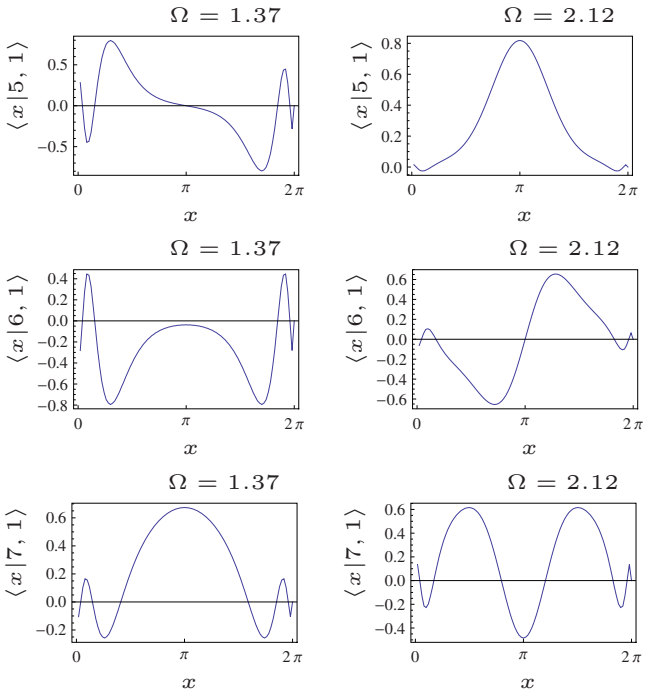

FIG. 11. (Color online) The first two Eigenfunctions of the Hamiltonian (22) for values of the oscillator parameter Ω before and after the level anticrossing.

previous system, however, we notice one feature, namely, the degeneracy of pairs of levels before the level anticrossing points. This degeneracy is due to the symmetry of the potential and indicates that the two degenerate states do not interact coherently, because they are localized above the two singularities of the potential, separated by the bulge in between. Interestingly, this degeneracy is lifted at those points where there is an anticrossing of both levels with the next higher band, pointing toward coherent tunneling between these states. In the following we will consider this level anticrossing region of the 5th and 6th states with the 7th state, cf. Fig. 10.

This view of the behavior of the eigenstates of the charged oscillator is clearly supported by the shape of the potential and the wave functions at the notable point of the level crossing, Fig. 11. The two degenerate states $|5,1\rangle$ and $|6,1\rangle$ are localized so deeply that they do not see each other through the potential hump, whereas the third state seems to be a remainder of the lowest harmonic oscillator state, being mainly localized in the metastable local minimum. As Ω increases, this parabolic minimum becomes more and more important until it becomes the prevalent feature of the potential. This means that there is less and less possibility for the lower states to be localized near the edges, so that they are finally pushed into the parabolic well where they form superpositions with the third state, finally resembling the usual harmonic oscillator states.

2. Transport

We apply our Master equation to this system, by coupling these three charged states to two empty states. Using the exact wave functions, we compute the FC factors. Due to the symmetry of the wave functions only three of the six possible transitions ($\{|1,0\rangle,|2,0\rangle\}\leftrightarrow\{|5,1\rangle,|6,1\rangle,|7,1\rangle\}$) have nonzero FC factors [cf. Figure 12]. We do not neglect the lower lying charged states, but their FC factors vanish for those Ω values we are considering here and thus they do not contribute to the transport, i.e., are FC blocked.

3. Results

In Fig. 13, we show the calculated noise spectrum scanning the oscillator parameter Ω through the level splitting point. To demonstrate the importance of the correct treatment of the FC factors, we compare the result we obtain using the correct FC factors to the noise spectra calculated when allowing the $|1,0\rangle\leftrightarrow|6,1\rangle$ transition that is otherwise forbidden due to a vanishing FC factor. Considering first the latter the case, where the FC blockade is lifted, we observe that for those Ω values where the two lower states are still degenerate, there is one single resonance corresponding to the energy difference between the degenerate and the third state. Con-

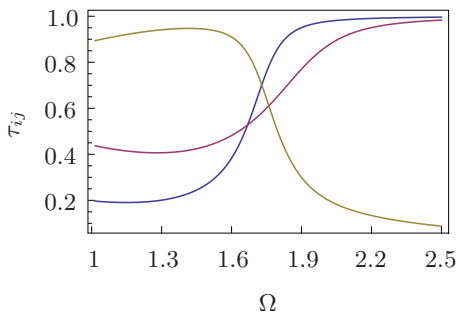

FIG. 12. (Color online) FC factors $\tau_{|5,1\rangle\leftrightarrow|1,0\rangle}$, $\tau_{|6,1\rangle\leftrightarrow|2,0\rangle}$ and $\tau_{|7,1\rangle\leftrightarrow|1,0\rangle}$. Only these three FC factors are nonzero, because for the others the product of wave functions under the integral is antisymmetric and hence vanishes when integrated over a symmetric interval.

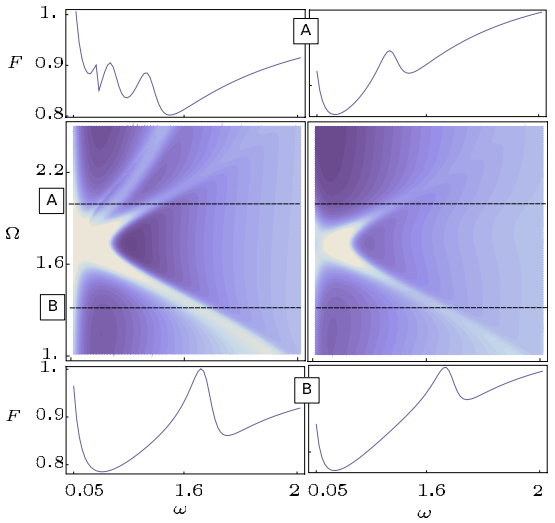

FIG. 13. (Color online) Frequency-dependent Fano factors $F(\omega)$ for different values of the oscillator parameter Ω. In the left panels, the transition $|1,0\rangle \leftrightarrow |6,1\rangle$ has been allowed by letting the corresponding FC factor $\tau_{|1,0\rangle\leftrightarrow|6,1\rangle}=0.1$. In the right panels, this transition is forbidden according to the correct treatment of the FC factors. The lines A and B indicate corresponding Ω values of the top and bottom panels, which can be seen as cuts through the two-dimensional plots.

sequently, this resonance occurs at smaller and smaller energies until the level splitting point is reached. After this point, the noise spectrum shows three resonances corresponding to interactions between all charged states $|5,1\rangle$, $|6,1\rangle$ and $|7,1\rangle$, which can be confirmed by comparing the level spacing of the charged states (Fig. 10) with the frequencies ω where the resonances occur. Turning now to the case where the $|1,0\rangle \leftrightarrow |6,1\rangle$ transition is blocked, we observe that the behavior before the splitting point is the same as for the other case, but that after this point, the peaks corresponding to interactions $|5,1\rangle \leftrightarrow |6,1\rangle$ and $|7,1\rangle \leftrightarrow |6,1\rangle$ are completely missing. The noise spectrum only shows the resonance between the states $|5,1\rangle$ and $|7,1\rangle$. Due to the FC blockade of this particular transition $|1,0\rangle \leftrightarrow |6,1\rangle$, no coherent interaction can take place between this state and the other charged states, although coherent interaction takes place when all states are charged form the same empty state. This very particular interplay between the noise peak and the FC blockade is visible only, because we used a Master equation that correctly accounts for the coherences and the FC factors.

IV. CONCLUSION

We have introduced a way of describing the effect of coupling between mechanical and electronic degrees of freedom on transport properties, by deriving a Master equation that rigorously includes the FC factors and keeps all coherences of the density operator. A main feature of this equation is that the sign of the FC factors has to be kept. We could show that the treatment of the coherences is essential to observe the internal dynamics of a nanomechanical system, where the electronic degree of freedom is coupled to the vibrational motion by considering the changing potential a quantum dot experiences under single electron transport due to electronic interaction with the environment. We considered two models for which we obtained the microscopically exact wave functions which have features known from two-level systems and used them to include damping of the vibrational motion into the model and calculate the exact FC factors. The role of the coherences becomes important when considering higher order transport properties, such as shot noise. Although the coherences vanish in the steady state solution for an undamped system, they are crucial for noise calculations, as we have shown by comparison to results we obtained omitting the coherences. Furthermore, the noise spectrum is extremely sensitive to FC blocked transitions as is accounts for all internal coherent tunneling processes and thus can indicate the absence of such interactions due to FC blockade. The damping of the vibrational motion has the expected effect of suppressing excited vibrational states, but its influence on the coherences is rather rich and merits, in our opinion, further investigation.

ACKNOWLEDGMENTS

Discussions with S. Gurvitz, F. v. Oppen, and M. Schultz are acknowledged. This work was supported by DFG under Grant No. 1528/5-1 and the WE Heraeus Foundation.

APPENDIX: BASIS FOR SYSTEM HAMILTONIAN OF MODEL I

The Hamiltonian (17) for the image charge system yields some similarities to the electronic Hamiltonian of the Hydrogen atom. In fact, for $\Omega=0$, it is exactly the radial part of the Hydrogen atom Hamiltonian for vanishing angular momentum $l=0$.[19] Therefore, we choose the eigenstates of this Hamiltonian

$$\psi_n(x) = \sqrt{\frac{(n-1)!}{2n(n!)}}\left(\frac{2\epsilon}{n}\right)^{3/2} e^{-\epsilon/nx} x L_{n-1}^1\left(\frac{2\epsilon}{n}x\right) \tag{A1}$$

as the basis set to represent the full Hamiltonian, i.e., for finite Ω values.

The diagonal matrix elements are

$$\langle\psi_n|H|\psi_n\rangle = -\frac{\epsilon^2}{2n^2} + \frac{\Omega^2}{2} - \frac{3\Omega^2}{2\epsilon}n^2 + \frac{\Omega^2}{4\epsilon^2}n^2(5n^2+1), \tag{A2}$$

and the off-diagonal elements

$$\begin{aligned}\langle\psi_n|\mathcal{H}|\psi_m\rangle &= \langle\psi_n|\Omega^2(1-x)^2|\psi_m\rangle \\ &= -\Omega^2\langle\psi_n|x|\psi_m\rangle + \frac{\Omega^2}{2}\langle\psi_n|x^2|\psi_m\rangle \\ &= -\Omega^2\sqrt{\frac{(n-1)!}{2n(n)!}}\left(\frac{2\epsilon}{n}\right)^{3/2}\sqrt{\frac{(m-1)!}{2m(m)!}}\left(\frac{2\epsilon}{m}\right)^{3/2}\int_0^\infty dx e^{-\epsilon/nx}xL_{n-1}^1\left(\frac{2\epsilon}{n}x\right)xe^{-\epsilon/mx}xL_{m-1}^1\left(\frac{2\epsilon}{m}x\right) \\ &+ \frac{\Omega^2}{2}\sqrt{\frac{(n-1)!}{2n(n)!}}\left(\frac{2\epsilon}{n}\right)^{3/2}\sqrt{\frac{(m-1)!}{2m(m)!}}\left(\frac{2\epsilon}{m}\right)^{3/2}\int_0^\infty dx e^{-\epsilon/nx}xL_{n-1}^1\left(\frac{2\epsilon}{n}x\right)x^2e^{-\epsilon/mx}xL_{m-1}^1\left(\frac{2\epsilon}{m}x\right) \qquad \text{(A3)}\end{aligned}$$

remain to be calculated. To this end we use the relation[29]

$$\int_0^\infty e^{-bx}x^\alpha L_n^\alpha(\lambda x)L_m^\alpha(\mu x)dx = \frac{\Gamma(m+n+\alpha+1)}{n!\,m!}\frac{(b-\lambda)^n(b-\mu)^m}{b^{m+n+\alpha+1}}\,{}_2F_1\left[-m,-n;-m-n-\alpha;\frac{b(b-\lambda-\mu)}{(b-\lambda)(b-\mu)}\right],$$

where ${}_2F_1$ is the Hypergeometric function. This is already very close to the integrals in Eq. (A3), if we identify

$$\alpha \to 1, \quad b \to \frac{\epsilon(n+m)}{nm}, \quad \lambda \to \frac{2\epsilon}{n}, \quad \mu \to \frac{2\epsilon}{m}. \qquad \text{(A4)}$$

However, we would like to have a x^3 and x^4 dependence. This is achieved by differentiating Eq. (A4) with respect to b

$$\begin{aligned}\partial_b\partial_b\int_0^\infty e^{-bx}x^\alpha L_n^\alpha(\lambda x)L_m^\alpha(\mu x)dx &= \int_0^\infty e^{-bx}x^{2+\alpha}L_n^\alpha(\lambda x)L_m^\alpha(\mu x)dx \\ &= \partial_b\partial_b\frac{\Gamma(m+n+\alpha+1)}{n!\,m!}\frac{(b-\lambda)^n(b-\mu)^m}{b^{m+n+\alpha+1}}\,{}_2F_1\left[-m,-n;-m-n-\alpha;\frac{b(b-\lambda-\mu)}{(b-\lambda)(b-\mu)}\right]\end{aligned}$$

$$\begin{aligned}\partial_b\partial_b\partial_b\int_0^\infty e^{-bx}x^\alpha L_n^\alpha(\lambda x)L_m^\alpha(\mu x)dx &= \int_0^\infty e^{-bx}x^{3+\alpha}L_n^\alpha(\lambda x)L_m^\alpha(\mu x)dx \\ &= \partial_b\partial_b\partial_b\frac{\Gamma(m+n+\alpha+1)}{n!\,m!}\frac{(b-\lambda)^n(b-\mu)^m}{b^{m+n+\alpha+1}}\,{}_2F_1\left[-m,-n;-m-n-\alpha;\frac{b(b-\lambda-\mu)}{(b-\lambda)(b-\mu)}\right]\end{aligned}$$

These expressions have to be normalized with the normalization factors of Eq. (A3). Thus, we have obtained an algebraic expression for the matrix elements of the Hamiltonian (17).

[1] C. W. J. Beenakker, Phys. Rev. B **44**, 1646 (1991).
[2] D. Weinmann, W. Häusler, W. Pfaff, B. Kramer, and U. Weiss, EPL **26**, 467 (1994).
[3] T. Brandes, Phys. Rep. **408**(5–6), 315 (2005).
[4] S. A. Gurvitz and Ya. S. Prager, Phys. Rev. B **53**, 15932 (1996).
[5] S. A. Gurvitz, Phys. Rev. B **57**, 6602 (1998).
[6] H. Park, J. Park, A. Lim, E. Anderson, A. Alivisatos, and P. McEuen, Nature (London) **407**, 57 (2000).
[7] R. G. Knobel and A. N. Cleland, Nature (London) **424**, 291 (2003).
[8] M. LaHaye, O. Buu, B. Camarota, and K. Schwab, Science **304**, 74 (2004).
[9] A. Naik, O. Buu, M. LaHaye, A. Armour, A. A. Clerk, and M. B. K. Schwab, Nature (London) **443**, 193 (2006).
[10] A. D. Armour, M. P. Blencowe, and K. C. Schwab, Phys. Rev. Lett. **88**, 148301 (2002).
[11] M. P. Blencowe, Phys. Rep. **395**, 159 (2004).
[12] J. Koch and F. von Oppen, Phys. Rev. Lett. **94**, 206804 (2005).
[13] J. Koch, M. E. Raikh, and F. von Oppen, Phys. Rev. Lett. **95**, 056801 (2005).
[14] J. Koch, F. von Oppen, and A. V. Andreev, Phys. Rev. B **74**, 205438 (2006).
[15] D. Fedorets, L. Y. Gorelik, R. I. Shekhter, and M. Jonson, Phys. Rev. Lett. **92**, 166801 (2004).
[16] A. D. Armour and A. MacKinnon, Phys. Rev. B **66**, 035333 (2002).
[17] T. Novotný, A. Donarini, and A.-P. Jauho, Phys. Rev. Lett. **90**, 256801 (2003).
[18] T. Novotný, A. Donarini, C. Flindt, and A.-P. Jauho, Phys. Rev. Lett. **92**, 248302 (2004).
[19] B. H. Bransden and C. J. Joachain, *Physics of Atoms and Molecules* (Prentice-Hall, Englewood Cliffs, NJ, 2005).
[20] H. Hübener and T. Brandes, Phys. Rev. Lett. **99**, 247206 (2007).
[21] J. Park, Nature (London) **417**, 722 (2002).
[22] S. Sapmaz, P. Jarillo-Herrero, Y. M. Blanter, C. Dekker, and H. S. J. van der Zant, Phys. Rev. Lett. **96**, 026801 (2006).
[23] V. Sazonova, Y. Xaish, H. Üstünel, D. Roundy, T. A. Arias, and P. L. McEuen, Nature (London) **431**, 284 (2004).

[24] R. Leturcq, C. Stampfer, K. Inderbitzin, L. Durrer, C. Hierold, E. Mariani, M. G. Schultz, F. von Oppen, and K. Ensslin, Nat. Phys. **5**, 327 (2009).
[25] E. M. Weig, R. H. Blick, T. Brandes, J. Kirschbaum, W. Wegscheider, M. Bichler, and J. P. Kotthaus, Phys. Rev. Lett. **92**, 046804 (2004).
[26] C. Flindt, T. Novotný, and A.-P. Jauho, EPL **69**, 475 (2005).
[27] C. Flindt, T. Novotný, and A.-P. Jauho, Physica E (Amsterdam) **29**, 411 (2005).
[28] A. Mitra, I. Aleiner, and A. J. Millis, Phys. Rev. B **69**, 245302 (2004).
[29] I. S. Gradshteyn, *Table of Integrals, Series and Products* (Academic Press, New York, 1994).
[30] M. Wagner, A. V. Chaplik, and U. Merkt, Phys. Rev. B **51**, 13817 (1995).
[31] D. Pfannkuche, V. Gudmundsson, and P. A. Maksym, Phys. Rev. B **47**, 2244 (1993).